NASA TECHNICAL NOTE

NASA TN D-6129

FLIGHT INVESTIGATION OF A V/STOL TRANSPORT MODEL WITH FOUR POD-MOUNTED LIFT FANS

by William A. Newsom, Jr., and Sue B. Grafton

Langley Research Center
Hampton, Va. 23365

0132983

1. Report No. NASA TN D-6129	2. Government Accession No.	3. Recipient's Catalog No.
4. Title and Subtitle FLIGHT INVESTIGATION OF A V/STOL TRANSPORT MODEL WITH FOUR POD-MOUNTED LIFT FANS		5. Report Date February 1971
		6. Performing Organization Code
7. Author(s) William A. Newsom, Jr., and Sue B. Grafton		8. Performing Organization Report No. L-7469
9. Performing Organization Name and Address NASA Langley Research Center Hampton, Va. 23365		10. Work Unit No. 721-01-11-06
		11. Contract or Grant No.
12. Sponsoring Agency Name and Address National Aeronautics and Space Administration Washington, D.C. 20546		13. Type of Report and Period Covered Technical Note
		14. Sponsoring Agency Code

15. Supplementary Notes
Technical film supplement L-1089 available on request.

16. Abstract

The investigation consisted of free-flight model tests in hovering and forward flight through the transition speed range up to the point where conversion would be made to wing-borne flight. Dynamic stability characteristics of the model were also calculated for correlation with flight results. Because of a small static margin and speed instability, artificial damping in pitch was needed to obtain satisfactory pitch characteristics. No problem was experienced with roll or yaw through the transition speed range.

17. Key Words (Suggested by Author(s)) Lift-fan V/STOL transport Transition tests Free flight	18. Distribution Statement Unclassified — Unlimited		
19. Security Classif. (of this report) Unclassified	20. Security Classif. (of this page) Unclassified	21. No. of Pages 31	22. Price* $3.00

FLIGHT INVESTIGATION OF A V/STOL TRANSPORT MODEL
WITH FOUR POD-MOUNTED LIFT FANS

By William A. Newsom, Jr., and Sue B. Grafton
Langley Research Center

SUMMARY

A flight investigation has been made in the Langley full-scale tunnel to study the stability and control characteristics of a model of a V/STOL transport airplane having four lift fans mounted in nacellelike pods on the wing. The investigation included hovering flight out of ground effect and forward flight through the transition speed range up to the speeds at which conversion would be made to wingborne flight. The dynamic stability characteristics of the model were also calculated for correlation with the results of the flight tests.

The hovering-flight tests out of ground effect showed that the controls-fixed motions of the model without artificial stabilization consisted of unstable oscillations in pitch and roll. In forward flight the model exhibited a simple divergence type of longitudinal instability because of a combination of small static margin and speed instability. The lateral-directional motions in the transition flight range were stable and the model was easily controllable. The use of artificial pitch-rate damping could stabilize the unstable pitching motions in hovering flight and make the configuration less unstable in the transition flight range, and the use of artificial roll-rate damping could stabilize the unstable rolling oscillations in hovering flight.

INTRODUCTION

Lift-fan configurations are of considerable interest for possible application to future V/STOL transport airplanes. Large-scale wind-tunnel investigations of a number of different configurations have been made at the NASA Ames Research Center to determine static aerodynamic characteristics, and the results of some of these investigations have been published in references 1 and 2. The NASA Langley Research Center is extending this research to determine the dynamic stability and control characteristics of a similar series of configurations.

The particular configuration covered herein has four lift fans mounted in nacellelike pods on a relatively straight wing. The investigation consisted of free-flight tests in the

Langley full-scale tunnel to determine the dynamic stability and control characteristics in the hovering and transition-flight conditions. The forward-flight speeds investigated covered the fan-powered flight range between hovering and the speed at which conversion would be made to wingborne flight. The conversion maneuver was not investigated but a few flights were made with the fans covered to examine the characteristics of the model when flying as a normal airplane. The results of the free-flight investigation were mainly qualitative and consisted of pilots' observations and opinions of the behavior of the model. The longitudinal and lateral-directional dynamic stability characteristics of the model were also calculated at several trim conditions for purposes of correlation with flight results. An extensive force-test investigation of this model was performed previously to define its aerodynamic characteristics, and the results are presented in reference 3.

SYMBOLS

Values are given in both SI and U.S. Customary Units. The measurements and calculations were made in U.S. Customary Units.

All forces and moments are referred to the body-axis system.

A,B,C,D,E   coefficients defined in appendixes A and B

c   local wing chord, m (ft)

$\bar{c}$ mean aerodynamic chord, m (ft)

$C_{1/2}$ cycles required for oscillation to damp to one-half amplitude

C_2 cycles required for oscillation to double amplitude

F_X force along X-body axis, N (lb)

F_Y force along Y-body axis, N (lb)

F_Z force along Z-body axis, N (lb)

g   acceleration due to gravity, m/sec^2 (ft/sec^2)

i_t tail incidence, deg

I_X moment of inertia about X-body axis, $kg\text{-}m^2$ ($slug\text{-}ft^2$)

2

I_Y moment of inertia about Y-body axis, $kg\text{-}m^2$ $(slug\text{-}ft^2)$

I_Z moment of inertia about Z-body axis, $kg\text{-}m^2$ $(slug\text{-}ft^2)$

$j = \sqrt{-1}$

m   mass, kg   (slugs)

M_X rolling moment, m-N   (ft-lb)

M_Y pitching moment, m-N   (ft-lb)

M_Z yawing moment, m-N   (ft-lb)

P   period of oscillation, sec

p   rolling velocity, rad/sec

q   pitching velocity, rad/sec

r   yawing velocity, rad/sec

S_h horizontal-tail area, m^2 (ft^2)

S_w wing area, m^2 (ft^2)

s Laplace operator, $\sigma + j\omega$, 1/sec

$t_{1/2}$ time required for mode of motion to damp to one-half amplitude, sec

$\dfrac{1}{t_{1/2}}$ damping parameter, 1/sec

t_2 time required for mode of motion to double amplitude, sec

u,v,w   perturbation velocities along X-, Y-, and Z-body axes, respectively, m/sec   (ft/sec)

U_0 trim velocity, m/sec   (ft/sec)

α angle of attack, deg or rad

β angle of sideslip, deg or rad

β_v fan-exit-vane angle, measured rearward from fan axis, deg

δ_f flap deflection, deg

ζ ratio of damping present in oscillatory mode of motion to value required for critical damping

θ angle of pitch, positive when nose is above horizon, deg or rad

σ real part of root of characteristic equation, 1/sec

ϕ angle of bank, deg or rad

ω imaginary part of root of characteristic equation, rad/sec

ω_n undamped natural frequency of oscillatory mode, rad/sec

Dimensional stability derivatives:

$$L_v = \frac{1}{I_X} \frac{\partial M_X}{\partial v} \qquad\qquad Y_v = \frac{1}{m} \frac{\partial F_Y}{\partial v}$$

$$L_p = \frac{1}{I_X} \frac{\partial M_X}{\partial \alpha} \qquad N_p = \frac{1}{I_Z} \frac{\partial M_Z}{\partial p} \qquad Y_p = \frac{1}{m} \frac{\partial F_Y}{\partial p}$$

$$L_r = \frac{1}{I_X} \frac{\partial M_X}{\partial r} \qquad N_r = \frac{1}{I_Z} \frac{\partial M_Z}{\partial r} \qquad Y_r = \frac{1}{m} \frac{\partial F_Y}{\partial r}$$

$$L_\beta = \frac{1}{I_X} \frac{\partial M_X}{\partial \beta} \qquad N_\beta = \frac{1}{I_Z} \frac{\partial M_Z}{\partial \beta}$$

$$M_u = \frac{I}{I_Y} \frac{\partial M_Y}{\partial u} \qquad M_w = \frac{1}{I_Y} \frac{\partial M_Y}{\partial w} \qquad M_q = \frac{1}{I_Y} \frac{\partial M_Y}{\partial q}$$

4

$$M_\alpha = \frac{1}{I_Y} \frac{\partial M_Y}{\partial \alpha}$$

$$X_u = \frac{1}{m} \frac{\partial F_X}{\partial u} \qquad\qquad X_w = \frac{1}{m} \frac{\partial F_X}{\partial w}$$

$$Z_u = \frac{1}{m} \frac{\partial F_Z}{\partial u} \qquad\qquad Z_w = \frac{1}{m} \frac{\partial F_Z}{\partial w}$$

APPARATUS AND TESTS

Model

General characteristics.- Photographs of the model used in the investigation are shown in figure 1, and a three-view drawing of the model is shown in figure 2. A list of the mass and geometric characteristics of the model is presented in table I. The four lift fans were mounted in nacellelike pods on the wing and were powered by compressed air driving turbine blades fixed on the circumference of the rotor. Each fan (the direction of rotation is indicated in fig. 2) was provided with a set of louver-type vanes mounted across the fan exits as shown in figure 3. The vanes were operated remotely and were used to redirect the fan slipstream for propulsion through the transition speed range. The wing trailing edge on each side of the fan pods could be removed and replaced by an alternate trailing edge having a single-slotted flap as shown in figure 3. When the undeflected trailing edge was in place, an aileron surface was present. For a few tests some large extensions to the T-mounted horizontal tail were used to increase the tail area from $0.30S_w$ to $0.40S_w$.

Controls.- For this investigation, jet-reaction controls were used about the three body axes of the model for attitude control, and height control was obtained by changing fan speed. Jets at the wing tips gave roll control, and jets at the tail gave yaw and pitch control.

The maximum jet-reaction control moments available and the accelerations produced by these moments are given in the following table:

Axis	Control moment		Acceleration, rad/sec^2
	m-N	ft-lb	
Pitch	25.5	(18.8)	1.9
Roll	14.0	(10.3)	2.0
Yaw	21.0	(15.5)	1.1

The ailerons, when mounted, and the rudder were interconnected to the roll and yaw control jets so that the aerodynamic surfaces operated to give a combination control whenever a control input was received (even in hovering flight).

The jet-reaction controls were operated by flicker-type (full-on or full-off) pneumatic mechanisms which were remotely operated by means of solenoid-operated valves. Each actuator had a motor-drive trimmer which was electrically operated so that controls could be rapidly trimmed independently of the flicker controls. The horizontal-tail incidence angle could be changed remotely and was considered to be the primary pitch trimming device.

Both the roll control and the pitch control were connected to a stability augmentation device. These devices consisted of roll-rate sensitive and pitch-rate sensitive gyroscopes that provided signals to servomechanisms connected to the roll control and pitch control which moved the controls to oppose a rolling or pitching motion.

Test Equipment and Setup

The setup for the free-flight tests made in the Langley full-scale tunnel is shown in figure 4. The model was flown in the 9- by 18-m (30- by 60-ft) open-throat test section of the tunnel and was remotely controlled about all three axes by human pilots. The pilots who controlled the model about its roll and yaw axes were located in an enclosure at the rear of the test section where they could best view the lateral-directional motions of the model. The pitch pilot, model power operator, and safety-cable operator were stationed at the side of the test section. Pneumatic and electric power and control signals were supplied to the model through the flexible trailing cable which was made up of wires and light plastic tubes. This trailing cable also incorporated a 0.318-cm (1/8-inch) steel cable that passed through a pulley above the test section. This cable was used as a safety cable to catch the model if an uncontrollable motion or mechanical failure occurred. The reasons for using this model flight technique in which the piloting duties are divided, in preference to the conventional single-pilot technique, is explained in detail in reference 4. In the tests made with fans covered (conventional airplane cruise) two pilots were used with one pilot controlling both roll and yaw and the other controlling pitch.

As a typical flight began, the model hung from the safety cable with zero tunnel airspeed. The tunnel drive motors were then started and the particular airspeed was established. The compressed-air power to the model fans was then increased and final adjustment made to the fan-exit vanes until the model was in equilibrium flight at the desired attitude and airspeed.

Tests

The investigation consisted of free-flight tests to determine the dynamic stability and control characteristics of the model during hovering flight out of ground effect and in fan-powered forward flight up to a speed of about 18.9 m/sec (62 ft/sec). This speed was approximately that at which final conversion to wingborne flight would be made. The conversion maneuver was not investigated owing to model mechanical limitations but a few flights were made with the fans covered to check the characteristics of the normal airplane configuration. Propulsion for these conventional flight tests was supplied by thrust from a compressed-air jet exhausting at the rear of the fuselage. The results of all tests were mainly qualitative and consisted of pilots' observations and opinions of the behavior of the model. Motion pictures were made of all flights for further study.

The hovering tests out of ground effect were performed by hovering the model at a height of 4.6 to 6.1 m (15 to 20 ft) above the ground board in the tunnel test section. In these tests the uncontrolled pitching and rolling motions and whether these motions could be stopped after they had been allowed to develop were examined. Forward flights were made at various fixed airspeeds to determine the stability and control characteristics of the model in the fan-powered flight range.

DYNAMIC STABILITY CALCULATIONS

The longitudinal and lateral-directional dynamic stability characteristics of the model were also calculated for correlation with the free-flight results. The linearized equations of motion used are presented in appendixes A and B. The aerodynamic data used in the calculations were based on the results of wind-tunnel tests presented in reference 3 and some additional unpublished results; these data are listed in table II. The results of the calculations are presented in terms of the period of an oscillation P and the damping parameter $\frac{1}{t_{1/2}}$. Positive values of $\frac{1}{t_{1/2}}$ denote stable modes of motion, whereas negative values of this parameter denote unstable modes of motion. The calculated results are listed in table III.

RESULTS AND DISCUSSION

A motion-picture supplement L-1089 has been prepared and is available on loan. A request card and a description of the film will be found at the back of this paper.

Hovering Flight

In hovering flight out of ground effect and without artificial stabilization, the model had unstable controls-fixed motions in both pitch and roll. Figure 5 shows time histories

of typical pitch and roll motions which were obtained from motion-picture records of flight tests in which the pilot held the control in a neutral position and allowed the motion to develop. Several attempts were made to obtain longer records, but the oscillation was so unstable that the safety cable was used to stop the model after only about three-quarters of a cycle. The longitudinal oscillation appeared to be a relatively low-frequency sliding motion, while the lateral oscillation was a higher frequency motion involving considerable rolling as well as lateral displacement. Although the model had unstable controls-fixed pitching and rolling motions, the pilots felt that the model was fairly easy to control because the period was sufficiently long and the initial rate of divergence was low. They could control the motions easily and the model could be flown fairly smoothly and could be maneuvered easily from one place to another. Although the model was easy to control without artificial stabilization, the pilots were aware of some disturbances from the slight random fluctuations in the recirculating fan slipstream in the tunnel area where the tests were made. No measurements except qualitative observations from persons standing in the test area have been made with this, or any other model, to determine the gustiness of the air in the test area. From such observations, however, it seems that the velocity changes involved in the disturbances are probably small compared with those that would be encountered outdoors on a gusty day, but they might have been more frequent than outdoor gust disturbances.

Hovering-flight tests were also made to study the effect of increased damping in roll and pitch on the hovering-flight characteristics of the model. In these tests it was found that the addition of artificial damping completely stabilized the model so that it no longer had an unstable oscillation. The use of artificial stabilization also reduced the response to the random disturbances to the point that the pilot effort needed to control the pitching and rolling motions was almost limited to making corrections to changes in trim.

The model had about neutral stability in yaw during hovering flights, and the only yaw control inputs required were those needed to keep the model properly oriented with respect to the various pilots. The yaw pilot had no difficulty in maintaining a constant heading during these hovering tests.

The calculated dynamic stability characteristics of the model for hovering flight are presented in table III. The longitudinal calculations were made for motion involving the two degrees of freedom shown in figure 5(a) (longitudinal displacement and pitch angle) and the lateral calculations were made for freedom in lateral displacement and roll angle. The results of the calculations agree with the free-flight results inasmuch as unstable oscillations were calculated for hovering flight. The unstable nature of the free-flight results limited the amount of information for correlation with the calculations, but the calculated results indicate a longer period for the longitudinal oscillation than for the lateral oscillation; this result is in agreement with the free-flight results. Also the

8

calculated period of the lateral oscillation of about 6 seconds seems to be approximately in agreement with the period indicated by the flight results of figure 5(b). The longitudinal flight record of figure 5(a), however, is entirely too short to provide even such an approximate correlation.

As pointed out in references 5 and 6, the frequency of the unstable oscillations in hovering flight is proportional to the values of L_v and M_u. The low frequency of the longitudinal oscillation was therefore probably caused by the relatively low value of M_u in hovering flight (see table II). Although not presented in table III, the results of additional calculations with increased damping in pitch M_q and damping in roll L_p indicated that the unstable oscillations could be made stable with about 10 times the basic values of L_p and M_q.

<center>Forward Flight</center>

The forward-flight tests were made in the steady level-flight condition for the flight range from hovering to a velocity of about 18.9 m/sec (62 ft/sec) (Lift coefficient ≈ 1.3). This speed corresponds approximately to the point at which conversion to wingborne flight would be made.

Test flights in the transition range were made for both the flap-undeflected and flap-deflected configurations. This was done because no attempt was made to determine optimum points in the transition for the flap to be deflected or undeflected. The flight characteristics of the model, other than performance, seemed in general to be independent of flap configuration, and except where specifically mentioned, the comments on stability characteristics apply to either flap configuration.

Longitudinal stability.- The basic stability of the model throughout the fan-powered flight range was determined during constant-airspeed flight tests with the model trimmed for flight at $\alpha = 0^o$. Examples of the types of motion experienced are shown in figure 6 which presents time histories of the control-fixed pitching motions for various airspeeds. This figure shows that the pitching motion in general became less severe with increase in forward speed but that the model appeared to be unstable in pitch in a simple divergence sense. The pilot considered the model difficult to fly because of this type of instability in that it kept diverging from the center of the test section and required constant attention to the longitudinal control. It was more troublesome than a model with the oscillatory type of instability encountered with some other types of V/STOL models, such as tilt-wing configurations, which required less frequent and close attention to longitudinal control to keep them flying in the center of the test section.

The apparent longitudinal instability of the model was investigated at some length because the static-force-test investigation of reference 3 and an unpublished dynamic-force-test investigation indicated no static longitudinal instability with respect to angle

of attack $\left(M_\alpha\ \text{positive}\right)$ or unstable damping in pitch $\left(M_q\ \text{positive}\right)$. An analysis of the data in reference 3 had indicated a possible problem resulting from speed instability; therefore a series of flight tests were made in which the angle of incidence of the horizontal tail was reduced so as to unload the tail and reduce the variation of pitching moment with velocity. The resulting loss of pitch trim was made up by the use of an auxiliary jet-reaction trimmer which was remotely controlled by the pitch pilot. It was found that when the pitch characteristics of the model were particularly bad $\left(\beta_V = 45^O,\ \delta_f = 0^O\right)$, a reduction of i_t from 13° to 3° gave very noticeable improvement in the apparent longitudinal stability. If, however, the model pitch problem was less serious $\left(\beta_V = 30^O,\ \delta_f = 0^O\right)$, a reduction of i_t did not produce a significant improvement in the apparent longitudinal stability. As a result of these tests, it was concluded that the speed instability of the model was not the major cause of the pitch problem. It was rationalized that the combination of speed instability and the very low static margin of the configuration, as mentioned in reference 3, was the cause of the pitch problem. Hence flight tests were made with the large tail extensions $\left(S_h = 0.40S_W\right)$, which provided a larger static margin, and showed that at the poor flight condition mentioned previously $\left(\beta_V = 45^O,\ \delta_f = 0^O\right)$, the model was very easy to fly and the pitch pilot was able to refrain from giving a control signal for several seconds at a time.

Since a horizontal tail with such a large span and area might be considered unreasonable, it was decided to investigate the use of artificial damping in pitch to improve the flight characteristics of the model. It was found that with the pitch-rate gyro in operation, the model was easy to fly through the entire transition speed range even with the stabilization system set to provide only a small proportion of the total control available.

During the flights in the conventional flight mode with the fans inoperative and covered, the pitch pilot found that the model flew well with no longitudinal stability trouble, and therefore artificial damping in pitch from the gyro system was not needed.

Calculated results of the dynamic longitudinal stability of the model over the transition flight range are presented in table III and figure 7. As pointed out in reference 5, in hovering flight the classical short-period oscillation becomes two real roots, one of which describes the vertical or height stability and one which describes an aperiodic convergence in pitch. The classical phugoid oscillation involving speed changes (longitudinal displacement) and pitch changes is the unstable oscillation in hovering flight. When the transition to forward flight has begun $\left(\beta_V = 20^O\right)$, the classical short-period oscillation appears, and although the period is relatively long, this mode of motion remains damped $\left(\dfrac{1}{t_{1/2}}\ \text{positive}\right)$ over the transition speed range. The existence of speed instability $\left(M_u\right.$ negative$\left.\right)$, however, causes the classical phugoid oscillation to become two aperiodic modes, one of which is unstable and is plotted in figure 7. This aperiodic divergence results from the negative values of M_u and relatively low values of M_α. The results

of the calculations therefore indicate statically unstable flight conditions in agreement with the free-flight test results. Additional calculations were made to verify the gains afforded by increased horizontal-tail area $(S_h = 0.40S_w)$ and pitch-rate damping for $\beta_V = 45^o$. As shown in table III, the increased horizontal-tail size (which increased the static margin from 2 percent to about 10 percent) was sufficient to stabilize the phugoid mode, and the model should have been dynamically stable, as was found in the flight tests. The effects of artificial damping in pitch on the unstable aperiodic mode of the basic model are shown in figure 8. As M_q is increased from -1.4 (basic value), the aperiodic mode becomes less unstable, but does not become dynamically stable. The gains noted in the free-flight tests are probably caused by the fact that pitch-rate damping made the mode less unstable to the point where the slightly divergent mode could not be distinguished from normal disturbances.

Lateral-directional stability.- In forward flight, the model was even easier to control in roll than it was in hovering flight. The fans provided a very high degree of damping in roll so that the pilots expressed the opinion that the rolling motion felt very nearly dead beat. Tests with the roll damper in operation showed that the added damping served to reduce the roll-pilot workload even though it was not actually needed for smooth easy flying.

The model had a high degree of directional stability and the yaw pilot had no difficulty in holding the model heading or in moving the model from place to place in the test section. No artificial stabilization was used in yaw at any time in the entire investigation.

When the flight tests were made in the conventional flight mode with the fans inoperative and covered, the yaw and roll controls were connected together electrically and operated as a coordinated control by one pilot. The model was easy to control in this condition and showed no problems with either static or dynamic lateral-directional stability.

The calculated lateral-directional dynamic stability characteristics are presented in table III and figure 9. As the transition to forward flight progresses, the results indicate that the unstable oscillation of hovering flight becomes stable between $\beta_V = 30^o$ and 45° in agreement with the free-flight tests, and that this oscillation becomes the Dutch roll oscillation in cruise flight.

Application of Results to Full-Scale Airplanes

There have been about 10 cases in which flight tests on V/STOL models in the wind tunnel such as the present series can be compared with flight tests of a full-scale airplane of the same configuration. On the basis of this experience it is possible to interpret some of the qualitative pilot evaluation of the handling qualities of the model in terms of its

significance to a full-scale airplane. The stability characteristics such as period and damping simply scale according to conventional scaling relations based on similar Froude number and relative-density factor.

The fact that the pilots of the model found it easy to fly in hovering flight in spite of the oscillatory instabilities in both pitch and roll is considered to indicate that a full-scale airplane would be easy to control in visual flight. Experience has shown, however, that a high degree of automatic stabilization is required for hovering flight on instruments. The pilot would not be expected to be aware of the fact that the model had unstable oscillations because the period of the oscillation is so long that he would sense the initial divergence and correct for it before it became apparent that the initial divergence would arrest itself and develop into an oscillation.

For the transition flight range, it is felt that the longitudinal instability, which appears as a speed instability, would be unacceptable and would have to be corrected for the airplane to be considered acceptable, even for visual flight. The lateral-directional characteristics, which were stable, are as good as or better than those of any V/STOL model previously tested and would be expected to be satisfactory for visual flight. Full-scale flight-test experience has shown, however, that no V/STOL airplane tested to date has had sufficient damping for flight on instruments; hence it can be assumed that the present configuration would also require substantial artificial stabilization for precision tasks such as final approach on instruments.

SUMMARY OF RESULTS

Free-flight model tests of a V/STOL transport airplane with four lift fans mounted in nacellelike pods on the wing yielded the following results:

1. Hovering-flight tests out of ground effect showed that the basic controls-fixed flight characteristic without artificial stabilization was an unstable oscillation in pitch and roll. The period of the oscillation was sufficiently long, however, so that the initial rate of divergence was low, and the model was reasonably easy to control in spite of the instability.

2. In forward flight, a combination of low static margin and speed instability caused an apparent dynamic longitudinal instability (simple divergence) which could be overcome by the use of artificial damping in pitch (pitch-rate damping).

3. A very high degree of roll damping existed through the entire transition speed range, and the roll pilot had no difficulty in controlling and maneuvering the model.

4. The model had a high degree of directional stability through the transition speed range, and the yaw pilot had no difficulty in controlling or maneuvering the model.

5. Calculated dynamic stability characteristics showed qualitative agreement with the results of the flight tests.

Langley Research Center,
        National Aeronautics and Space Administration,
                Hampton, Va., January 13, 1971.

APPENDIX A

LONGITUDINAL EQUATIONS OF MOTION

The linearized small-perturbation longitudinal equations of motion used were:

Vertical force

$$-Z_u u + \left(s - Z_w\right)w - U_o s\theta = 0 \tag{A1}$$

Longitudinal force

$$\left(s - X_u\right)u - X_w w + g\theta = 0 \tag{A2}$$

Pitching moment

$$-M_u u - M_w w + \left(s^2 - M_q s\right)\theta = 0 \tag{A3}$$

For nontrivial solutions, s must be a root of the characteristic equation

$$As^4 + Bs^3 + Cs^2 + Ds + E = 0 \tag{A4}$$

where

$A = 1$

$B = -M_q - X_u - Z_w$

$C = -M_w U_o + X_u\left(Z_w + M_q\right) + M_q Z_w - Z_u X_w$

$D = M_w U_o X_u + X_w\left(M_q Z_u - U_o M_u\right) + gM_u - M_q Z_w X_u$

$E = g\left(Z_u M_w - M_u Z_w\right)$

The damping and period of a mode of motion, in seconds, are given by the equations $t_{1/2} = -\dfrac{0.693}{\sigma}$ and $P = \dfrac{2\pi}{\omega}$, respectively, where σ and ω are the real and imaginary parts of the root of the characteristic equation. Additional stability characteristics may be obtained by the relations

$$\left. \begin{aligned} C_{1/2} &= \frac{t_{1/2}}{P} \\[2mm] \omega_n &= \sqrt{\sigma^2 + \omega^2} \\[2mm] \zeta &= -\frac{\sigma}{\omega_n} \end{aligned} \right\} \tag{A5}$$

APPENDIX B

LATERAL-DIRECTIONAL EQUATIONS OF MOTION

The linearized small-perturbation lateral-directional equations of motion used were:

Side force

$$\left(s - Y_v\right)\beta + \left(-sY_p - \frac{g}{U_o}\right)\phi + \left(-Y_r + 1\right)r = 0 \tag{B1}$$

Rolling moment

$$-L_\beta\beta + \left(s^2 - sL_p\right)\phi - L_r r = 0 \tag{B2}$$

Yawing moment

$$-N_\beta\beta - sN_p\phi + \left(s - N_r\right)r = 0 \tag{B3}$$

where

$$\beta = \frac{v}{u_o}$$

For nontrivial solutions, s must be a root of the characteristic equation

$$As^4 + Bs^3 + Cs^2 + Ds + E = 0 \tag{B4}$$

where

$A = 1$

$B = -Y_v - L_p - N_r$

$C = N_\beta + L_pN_r - L_rN_p + Y_v\left(L_p + N_r\right) - L_\beta Y_p - N_\beta Y_r$

$D = L_\beta N_p - L_pN_\beta - Y_v\left(L_pN_r - L_rN_p\right) - \frac{g}{U_o}L_\beta - L_\beta\left(Y_rN_p - N_rY_p\right) + N_\beta\left(Y_rL_p - L_rY_p\right)$

$E = \frac{g}{U_o}\left(L_\beta N_r - L_rN_\beta\right)$

The damping and period of a mode of motion, in seconds, are given by the equations $t_{1/2} = -\frac{0.693}{\sigma}$ and $P = \frac{2\pi}{\omega}$, respectively, where σ and ω are the real and imaginary parts of the roots of the stability equation. Additional stability characteristics may be obtained by the relations

$$C_{1/2} = \frac{t_{1/2}}{P}$$

$$\omega_n = \sqrt{\sigma^2 + \omega^2}$$

$$\zeta = -\frac{\sigma}{\omega_n}$$

(B5)

REFERENCES

1. Hall, Leo P.; Hickey, David H.; and Kirk, Jerry V.:   Aerodynamic Characteristics of a Large-Scale V/STOL Transport Model With Lift and Lift-Cruise Fans. NASA TN D-4092, 1967.

2. Kirk, Jerry V.; Hodder, Brent K.; and Hall, Leo P.:   Large-Scale Wind-Tunnel Investigation of a V/STOL Transport Model With Wing-Mounted Lift Fans and Fuselage-Mounted Lift-Cruise Engines for Propulsion. NASA TN D-4233, 1967.

3. Newsom, William A., Jr.:   Wind-Tunnel Investigation of a V/STOL Transport Model With Four Pod-Mounted Lift Fans. NASA TN D-5942, 1970.

4. Parlett, Lysle P.; and Kirby, Robert H.:   Test Techniques Used by NASA for Investigating Dynamic Stability Characteristics of V/STOL Models. J. Aircraft, vol. 1, no. 5, Sept.-Oct. 1964, pp. 260-266.

5. Chambers, Joseph R.; and Grafton, Sue B.:   Calculation of the Dynamic Longitudinal Stability of a Tilt-Wing V/STOL Aircraft and Correlation With Model Flight Tests. NASA TN D-4344, 1968.

6. Chambers, Joseph R.; and Grafton, Sue B.:   Investigation of Lateral-Directional Dynamic Stability of a Tilt-Wing V/STOL Transport. NASA TN D-5637, 1970.

TABLE I.- MASS AND GEOMETRIC CHARACTERISTICS OF MODEL

Weight, N (lb) 378 (85)

Moment of inertia:
   I_X, kg-m^2 (slug-ft^2) 6.897 (5.087)
   I_Y, kg-m^2 (slug-ft^2) 13.363 (9.856)
   I_Z, kg-m^2 (slug-ft^2) 18.846 (13.900)

Fuselage:
   Length, cm (ft) 223.4 (7.33)
   Cross-sectional area, max., cm^2 (ft^2) 1244.9 (1.34)

Wing:
   Area, cm^2 (ft^2) 12866.6 (13.85)
   Span, cm (ft) 228.0 (7.48)
   Aspect ratio 4.05
   Mean aerodynamic chord, cm (ft) 57.6 (1.89)
   Tip chord, cm (ft) 42.4 (1.39)
   Root chord, cm (ft) 70.7 (2.32)
   Taper ratio 0.60
   Dihedral angle, deg 0
   Thickness ratio 0.15
   Airfoil section . . . . Clark YH
   Aileron, each:
      Chord, percent wing chord 20
      Area, cm^2 (ft^2) 343.7 (0.37)
   Flap, each:
      Type . . . . Single slotted
      Chord, percent wing chord 30
      Span:
         Inboard section, cm (ft) 26.8 (0.88)
         Outboard section, cm (ft) 41.1 (1.35)

Fans:
   Diameter, cm (ft) 20.3 (0.667)
   Exit-vane chord, cm (ft) 2.8 (0.092)
   Number of vanes 9

Vertical tail:
   Area, cm^2 (ft^2) 1932.3 (2.08)
   Span, cm (ft) 48.8 (1.60)
   Aspect ratio 1.23
   Root chord, cm (ft) 49.7 (1.63)
   Tip chord, cm (ft) 29.9 (0.98)
   Airfoil section . . . . NACA 0012
   Rudder:
      Chord, cm (ft) 8.8 (0.29)
      Span, cm (ft) 46.3 (1.52)
   Tail length, c.g. to 0.25$\overline{c}$, cm (ft) 94.5 (3.10)

Horizontal tail:
   Area, cm^2 (ft^2) 3864.6 (4.16)
   Span, cm (ft) 147.2 (4.83)
   Aspect ratio 5.60
   Root chord, cm (ft) 35.7 (1.17)
   Tip chord, cm (ft) 16.8 (0.55)
   Taper ratio 0.47
   Dihedral angle, deg 0
   Pivot position . . . . 0.39 root chord
   Airfoil section . . . . NACA 0012
   Elevator, each:
      Root chord, cm (ft) 10.7 (0.35)
      Tip chord, cm (ft) 6.4 (0.21)
      Span, cm (ft) 56.7 (1.86)
   Tail length, c.g. to 0.25$\overline{c}$, cm (ft) 104.5 (3.43)

TABLE II.- STABILITY DERIVATIVES

(a) Longitudinal

β_v, deg	U_o		X_u	X_w	Z_u	Z_w	M_u		M_w		M_q
	m/sec	ft/sec	per sec	per sec	per sec	per sec	per m-sec	per ft-sec	per m-sec	per ft-sec	per rad-sec
0	0	0	-0.1992	0	0	0	0.0331	0.0101	0	0	-0.0375
20	11.6	38.0	-.3448	-.1147	-.5096	-1.0712	-.1732	-.0528	.0971	.0296	-.6917
30	12.8	42.0	-.2874	.2347	-.5939	-1.5945	-.2031	-.0619	-.0026	-.0008	-1.0153
45	15.9	52.0	-.3142	.1488	-.9195	-2.0680	-.3610	-.0110	-.0617	-.0188	-1.4121
45 ($S_h = 0.40S_w$)	15.9	52.0	-.3142	.1488	-.9195	-2.0680	-.3610	-.0110	-.3084	-.0940	-1.8359

(b) Lateral

β_v, deg	U_o		Y_v	Y_p		Y_r		L_β	L_p	L_r	N_β	N_p	N_r
	m/sec	ft/sec	per sec	m/sec	ft/sec	m/sec	ft/sec	per sec^2	per sec	per sec	per sec^2	per sec	per sec
0	0	0	-0.1034	0	0	0	0	*-0.0725	-1.3809	0	0	0	0
20	11.6	38.0	-.3000	0	0	0	0	-8.2797	-1.4882	1.1575	1.6909	-.0605	-.3752
30	12.8	42.0	-.3503	0	0	0	0	-8.4500	-1.9314	1.3906	2.3654	-.0707	-.3958
45	15.9	52.0	-.4316	0	0	0	0	-12.5160	-2.6172	1.4989	4.4424	-.0731	-.3831
Cruise	26.5	87.0	-.4663	0	0	0	0	-19.9600	-3.1517	3.4669	8.4518	-.0577	-.9227

*Value given for $\beta_v = 0$ is L_v $\left(L_\beta$ is undefined for $U_o = 0\right)$.

TABLE III.- SUMMARY OF CALCULATED DYNAMIC STABILITY CHARACTERISTICS

β_V, deg	Mode	σ, 1/sec	ω, rad/sec	$t_{1/2}$, sec (*)	P, sec	$C_{1/2}$ (*)	ω_n, rad/sec	ζ (*)
Longitudinal
0	Oscillatory	0.268	±0.59	-2.58	10.62	-0.24	0.65	-0.413
	Aperiodic	-.773	0	.90	----	----	---	-----
↓	Aperiodic	0	0	∞	----	----	---	-----
20	Oscillatory	-.731	±.80	.94	7.83	.12	1.08	.674
	Aperiodic	-1.758	0	.57	----	----	---	-----
↓	Aperiodic	1.113	0	-.62	----	----	---	-----
30	Oscillatory	-.965	±1.10	.72	5.70	.13	1.46	.659
	Aperiodic	-1.789	0	.39	----	----	---	-----
↓	Aperiodic	.822	0	-.84	----	----	---	-----
45	Oscillatory	-1.737	±1.02	.39	6.15	.06	2.01	.862
	Aperiodic	-.422	0	1.64	----	----	---	-----
↓	Aperiodic	.102	0	-6.77	----	----	---	-----
45 $\left(S_h = 0.40 S_w\right)$	Oscillatory	-.090	±.49	7.68	12.72	.60	.50	.18
	Oscillatory	-1.807	±2.21	.38	2.85	.13	2.85	.63
Lateral directional
0	Oscillatory	0.257	±1.05	-2.70	5.98	-0.45	1.08	-0.245
	Aperiodic	-2.000	0	-0.35	----	----	---	-----
↓	Aperiodic	0	0	∞	----	----	---	-----
20	Oscillatory	.241	±1.96	-2.87	3.20	-1.12	1.98	-.122
	Aperiodic	-2.548	0	0.27	----	----	---	-----
↓	Aperiodic	-.098	0	7.09	----	----	---	-----
30	Oscillatory	.048	±2.07	-1.42	3.03	-.21	2.07	-.023
	Aperiodic	-2.771	0	.25	----	----	---	-----
↓	Aperiodic	-.003	0	194.69	----	----	---	-----
45	Oscillatory	-.095	±2.53	7.31	2.48	.34	2.53	.037
	Aperiodic	-3.297	0	.21	----	----	---	-----
↓	Aperiodic	.054	0	-12.72	----	----	---	-----
Cruise	Oscillatory	-.487	±3.18	1.42	1.97	1.39	3.22	.151
	Aperiodic	-3.672	0	.19	----	----	---	----
↓	Aperiodic	.105	0	-6.56	----	----	---	-----

*Negative signs indicate unstable modes of motion. For example, if $t_{1/2} = -2.70$, then $t_2 = 2.70$ or if $C_{1/2} = -0.45$, then $C_2 = 0.45$.

20
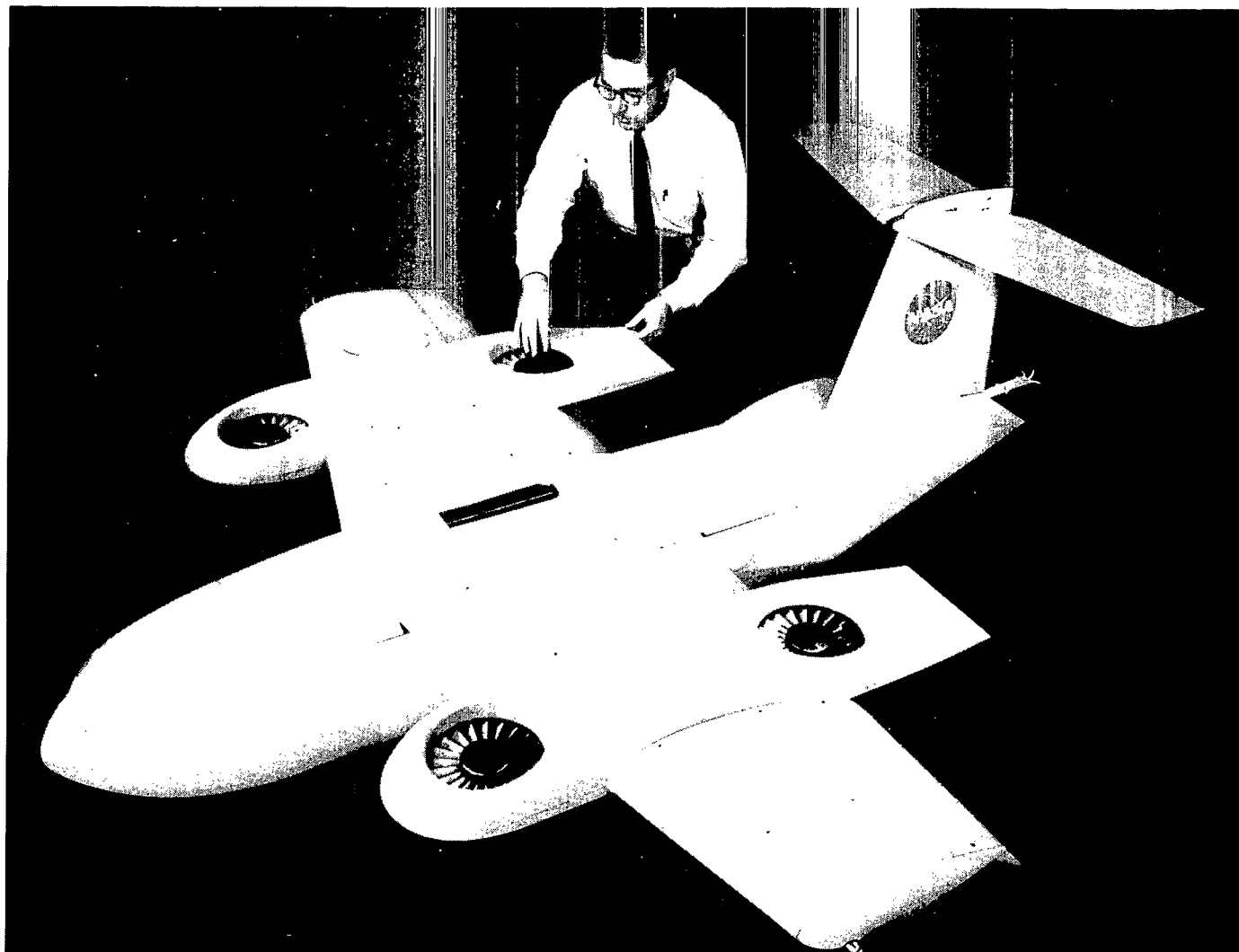
L-67-7754

(a) Three-quarter front view.

Figure 1.- Photographs of model.
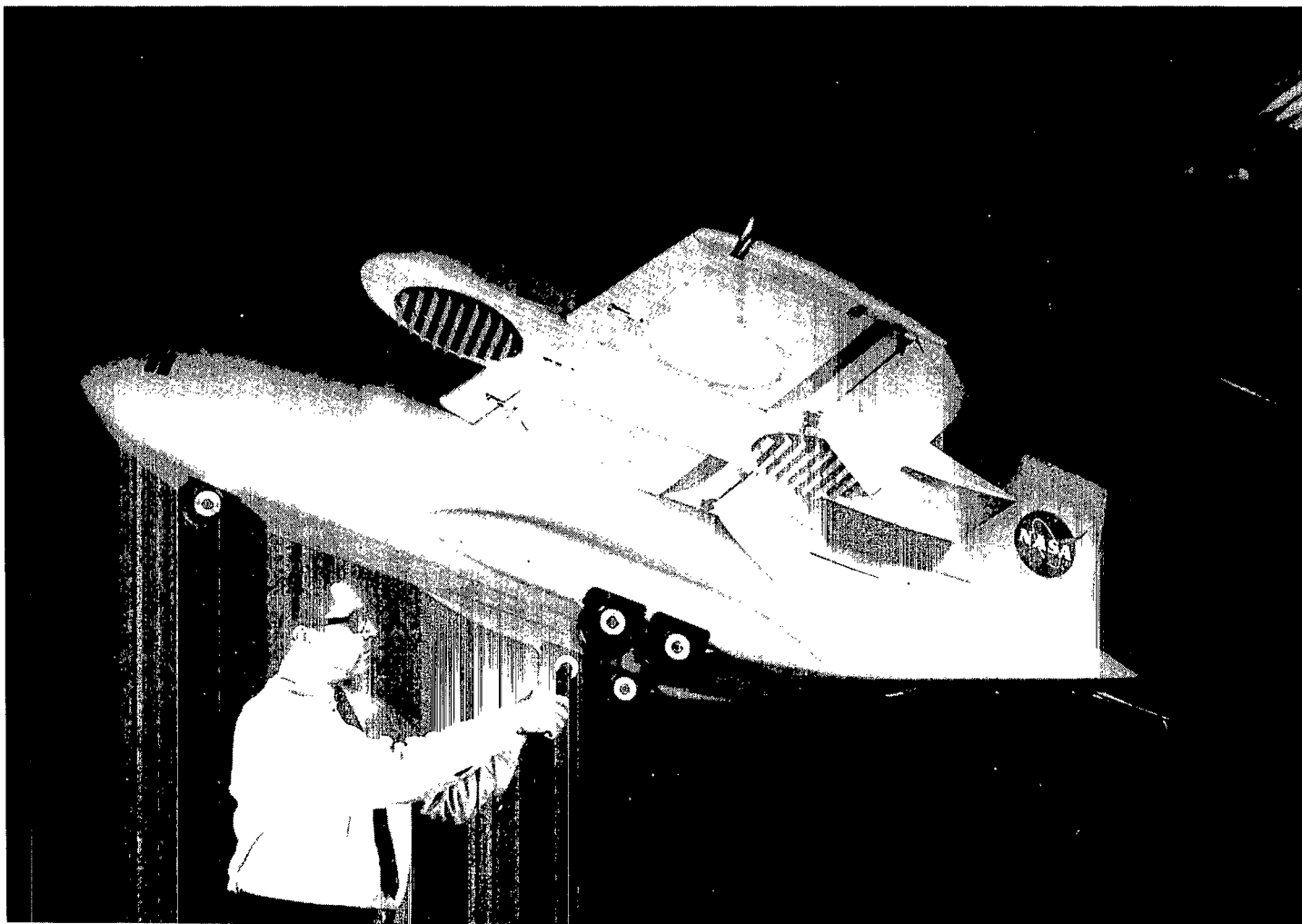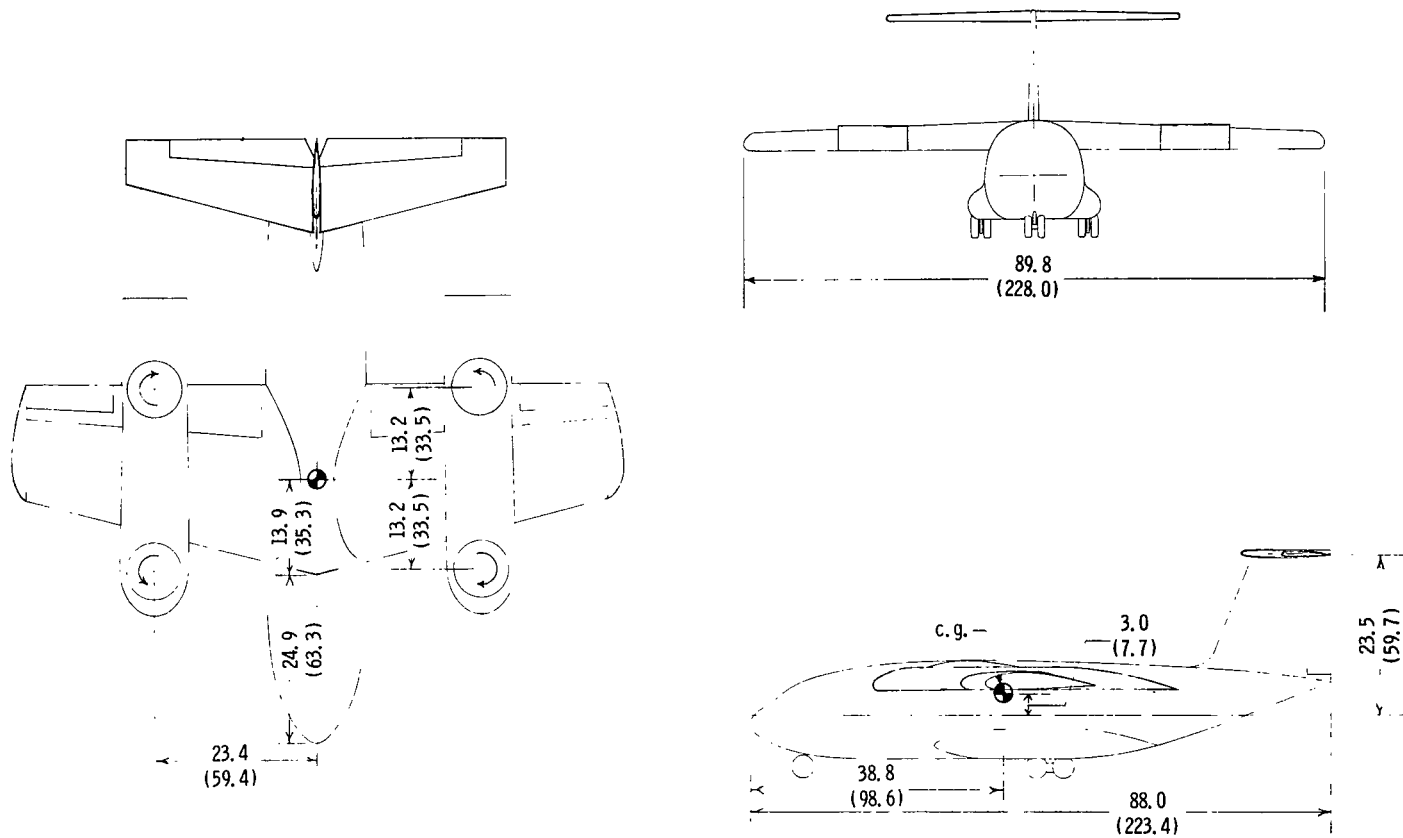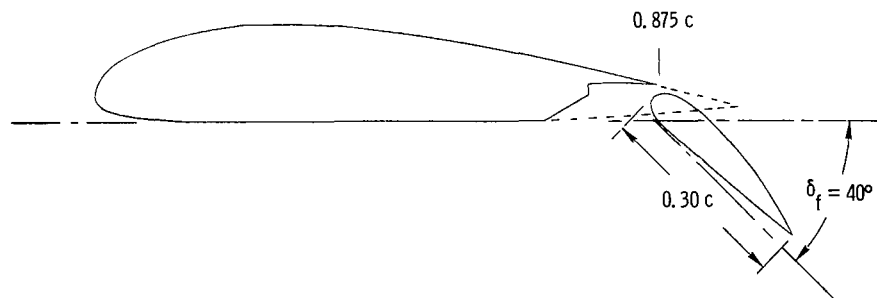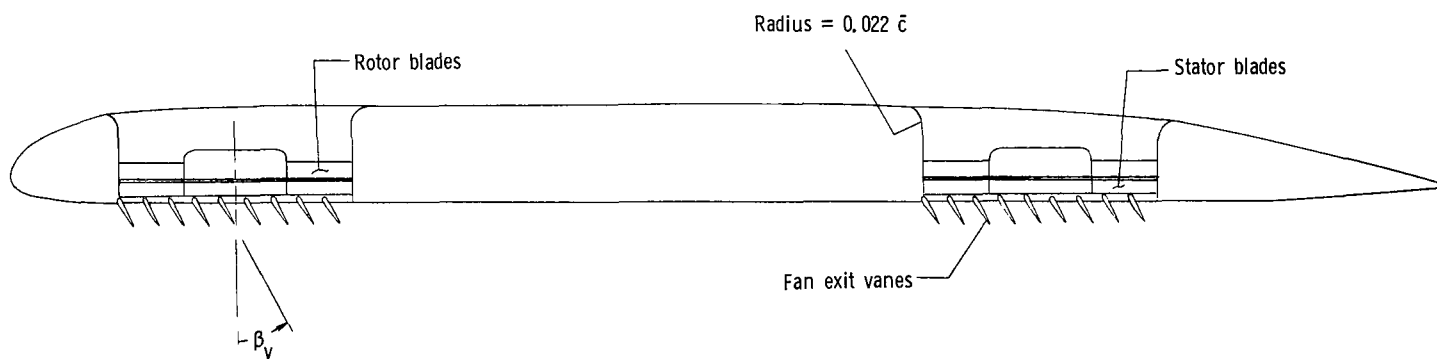
L-67-7757

(b) Bottom view.

Figure 1.- Concluded.

Figure 2.- Sketch of model. Dimensions are given first in inches and parenthetically in centimeters.

0.875 c

$\delta_f = 40°$

0.30 c

(a) Typical section through wing showing flap detail.

Radius = 0.022 $\bar{c}$

Rotor blades

Stator blades

Fan exit vanes

β_v

(b) Section through pod showing lift-fan position.

Figure 3.- Sketch showing wing and lift-fan pod details.
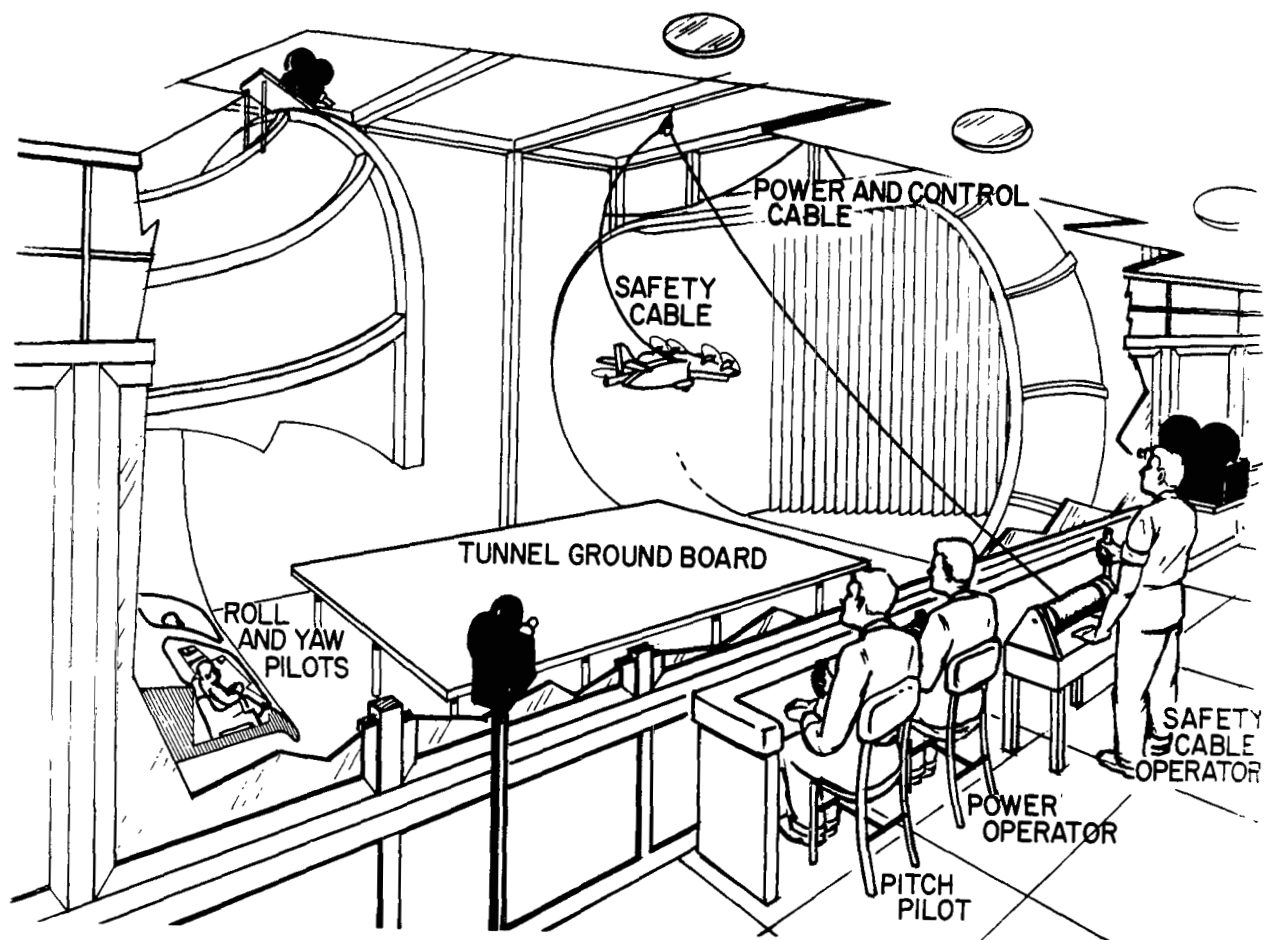
Figure 4.- Setup for flight tests in Langley full-scale tunnel.

Labels in figure:
- POWER AND CONTROL CABLE
- SAFETY CABLE
- TUNNEL GROUND BOARD
- ROLL AND YAW PILOTS
- SAFETY CABLE OPERATOR
- POWER OPERATOR
- PITCH PILOT
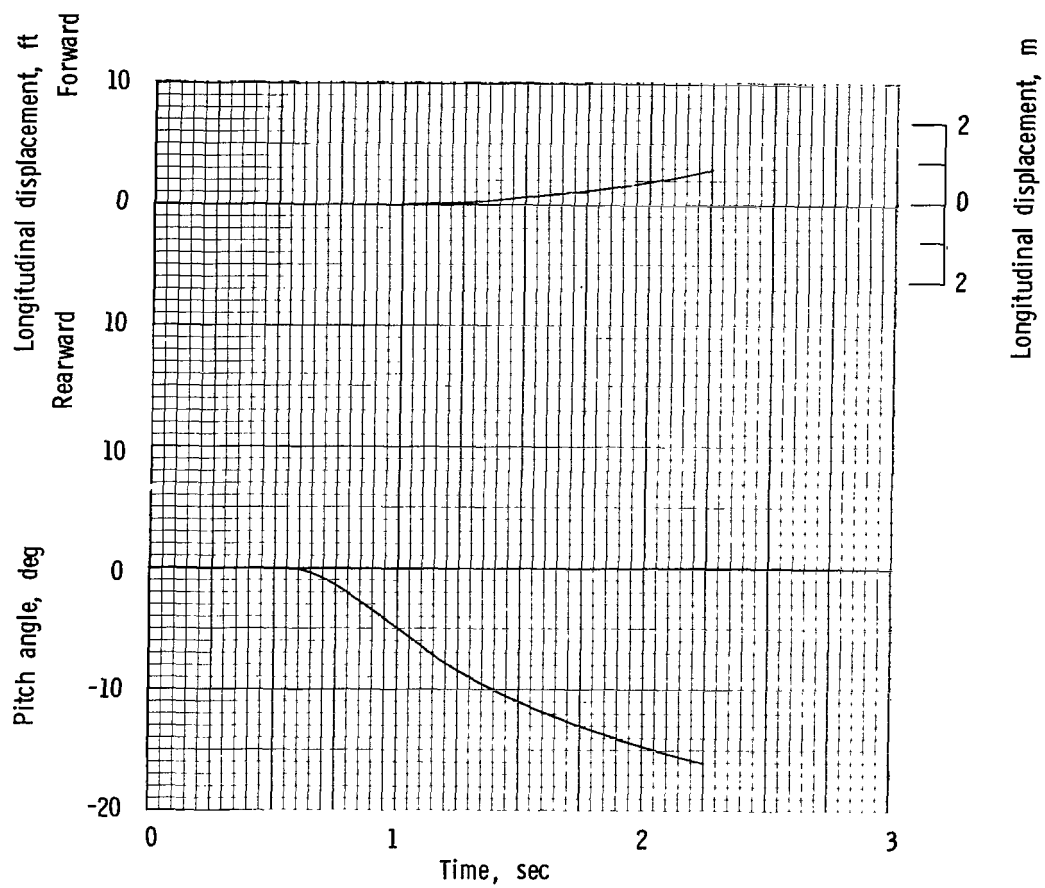
(a) Longitudinal.

Figure 5.- Typical controls-fixed motions of model in hovering flight.
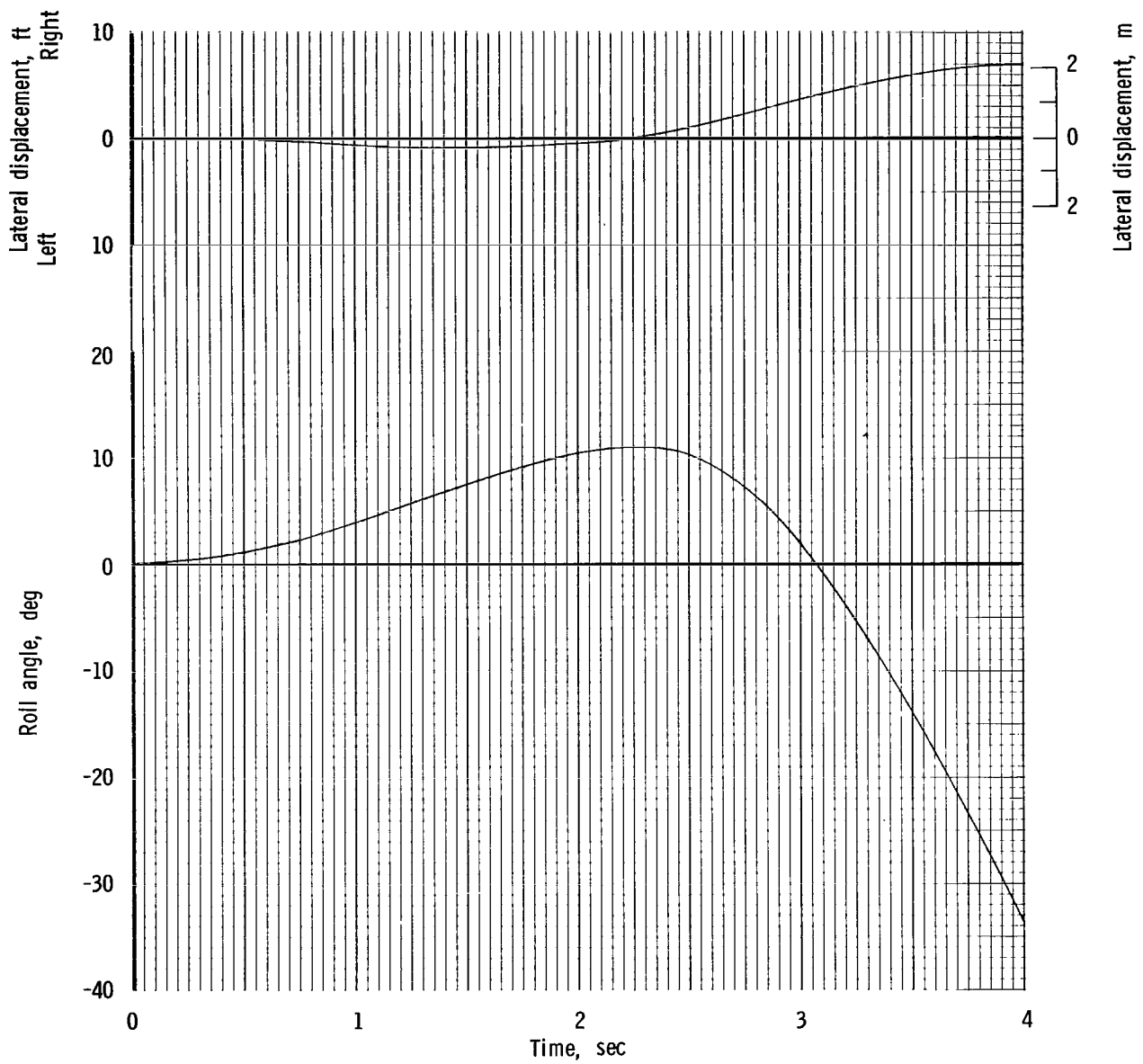
(b) Lateral.

Figure 5.- Concluded.
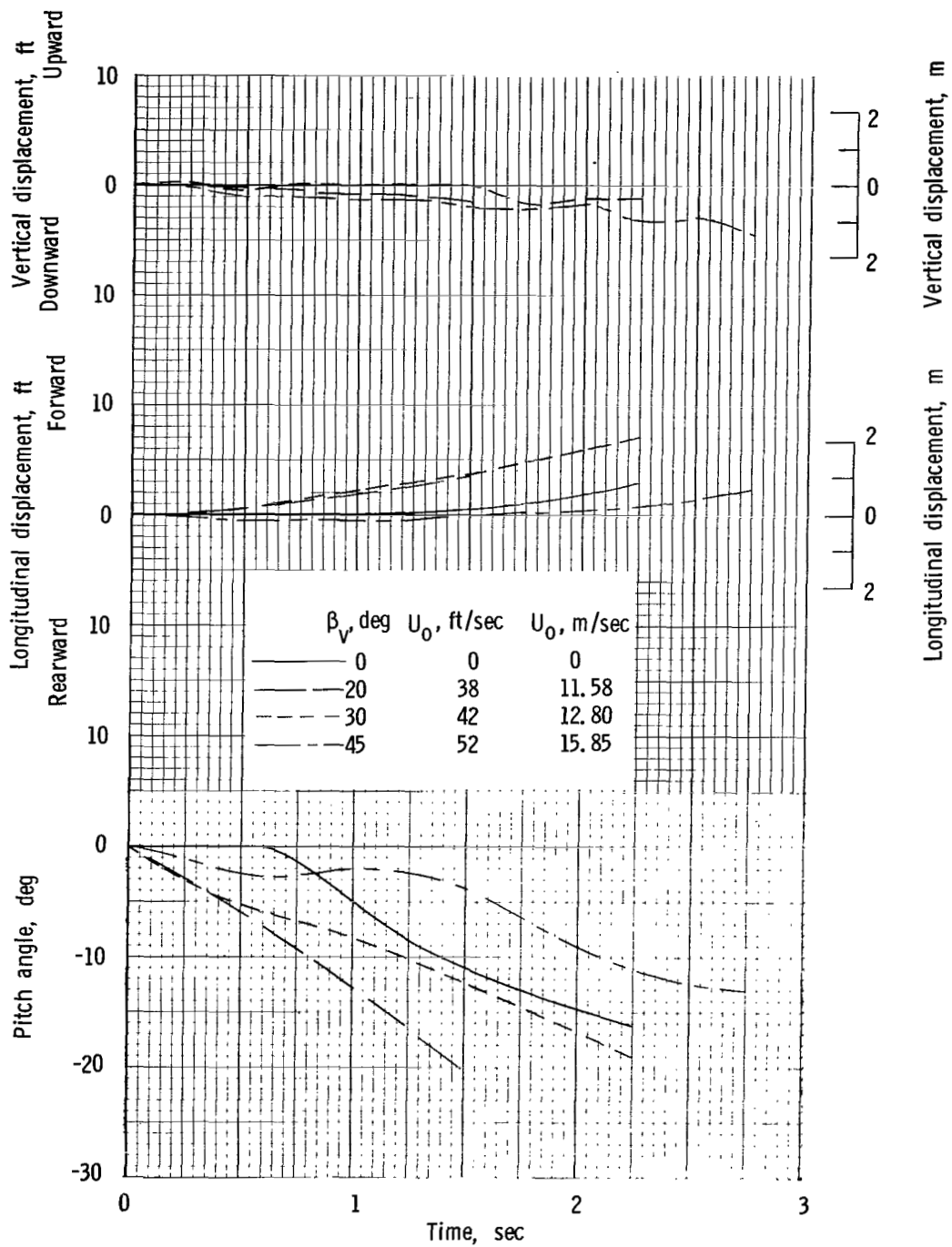
Figure 6.- Typical control-fixed longitudinal motions of model at several forward speeds in transition range. $\delta_f = 40^O$.
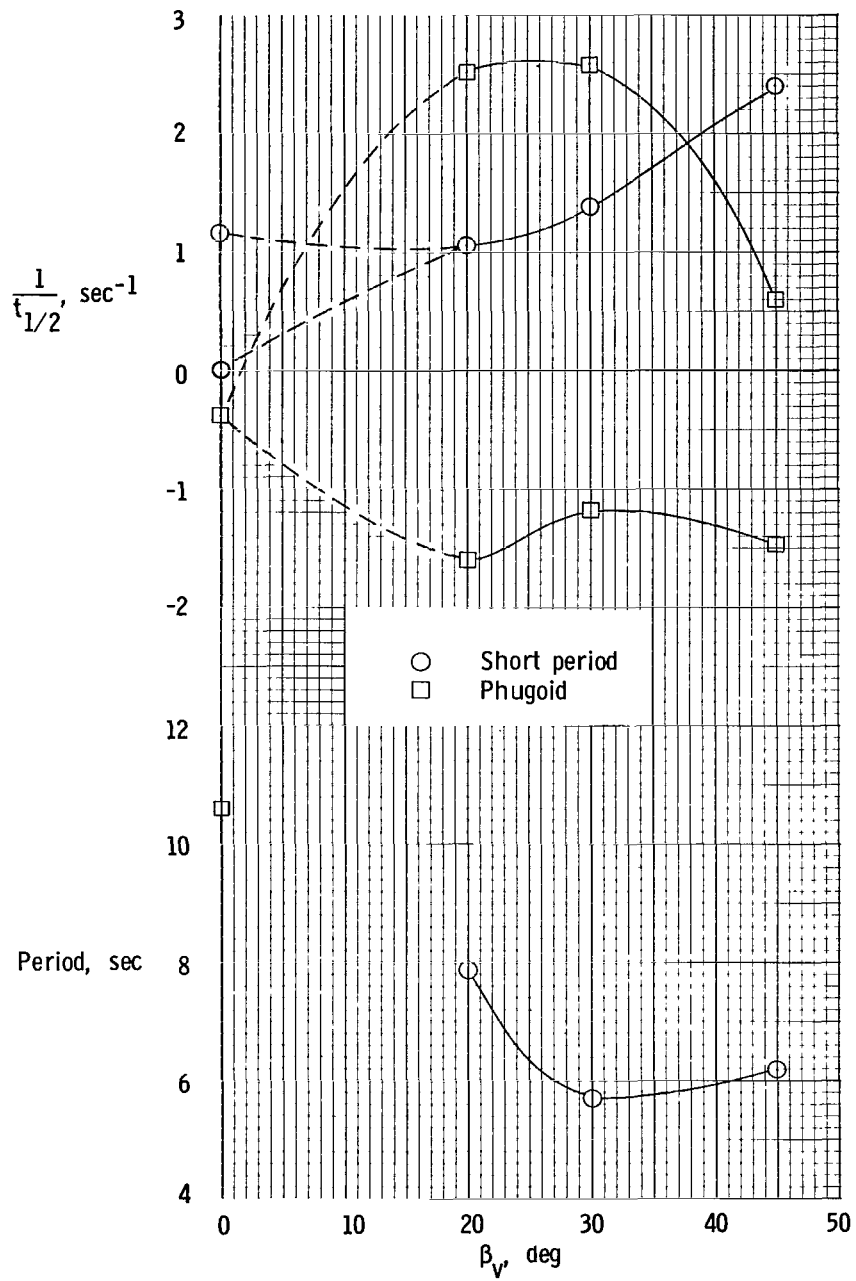
Figure 7.- Calculated characteristics of longitudinal oscillations.
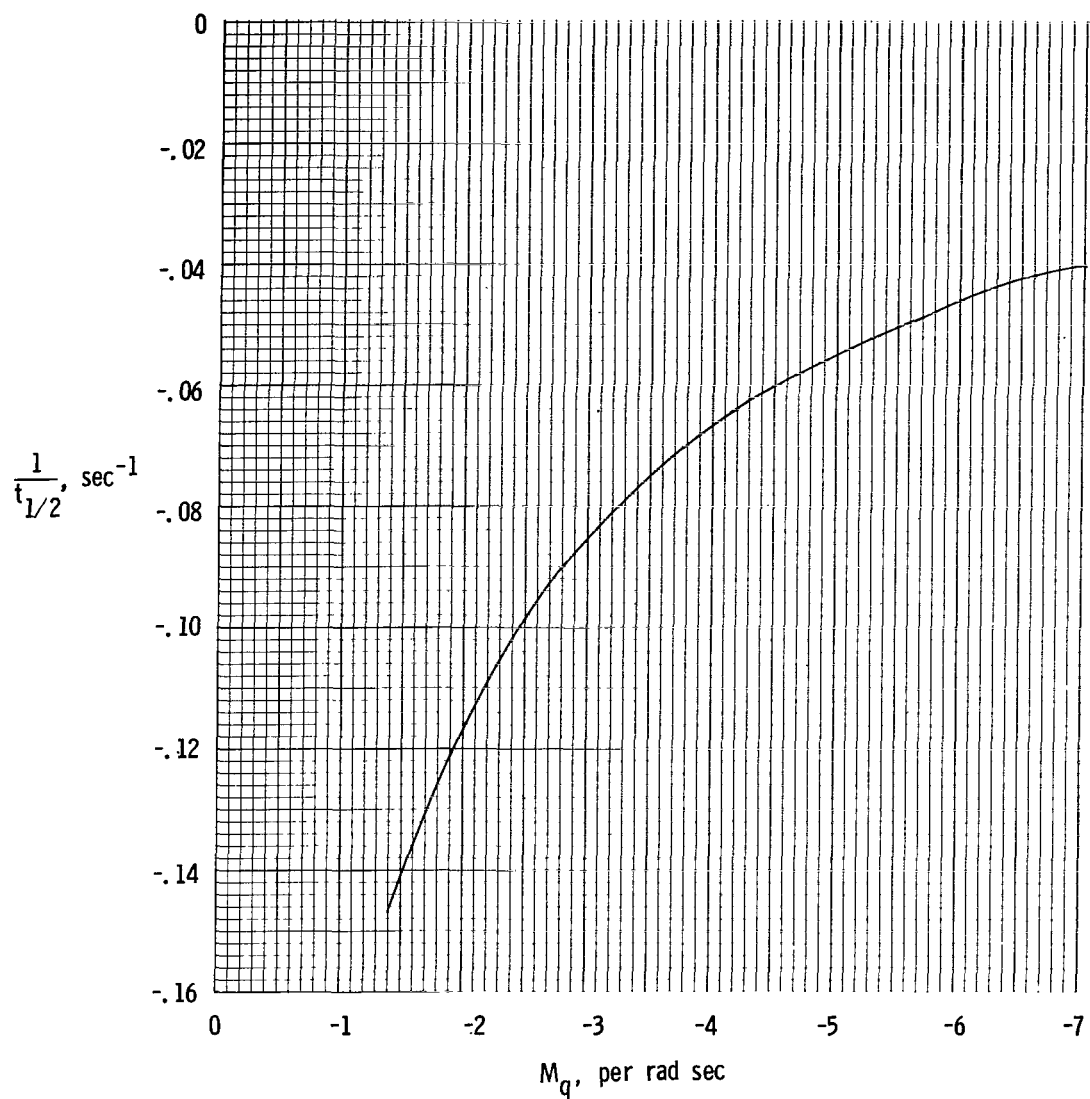
Figure 8.- Effect of artificial damping in pitch on calculated unstable aperiodic mode of basic model. $\beta_V = 45^O$; $U_O = 15.9$ m/sec (52 ft/sec).
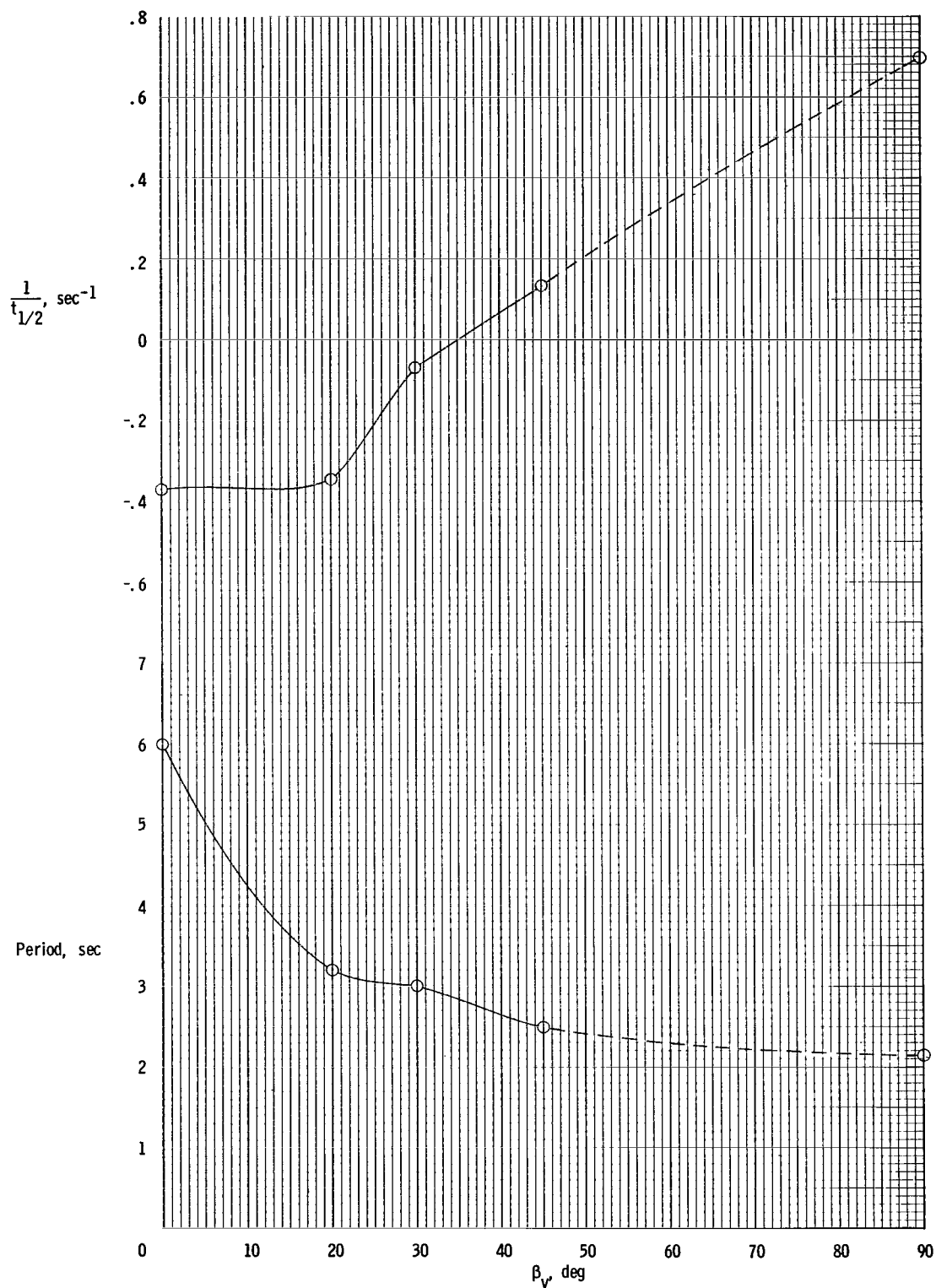
Figure 9.- Calculated characteristics of lateral-directional oscillations.

"The aeronautical and space activities of the United States shall be conducted so as to contribute . . . to the expansion of human knowledge of phenomena in the atmosphere and space. The Administration shall provide for the widest practicable and appropriate dissemination of information concerning its activities and the results thereof."

— NATIONAL AERONAUTICS AND SPACE ACT OF 1958

NASA SCIENTIFIC AND TECHNICAL PUBLICATIONS

TECHNICAL REPORTS: Scientific and technical information considered important, complete, and a lasting contribution to existing knowledge.

TECHNICAL NOTES: Information less broad in scope but nevertheless of importance as a contribution to existing knowledge.

TECHNICAL MEMORANDUMS: Information receiving limited distribution because of preliminary data, security classification, or other reasons.

CONTRACTOR REPORTS: Scientific and technical information generated under a NASA contract or grant and considered an important contribution to existing knowledge.

TECHNICAL TRANSLATIONS: Information published in a foreign language considered to merit NASA distribution in English.

SPECIAL PUBLICATIONS: Information derived from or of value to NASA activities. Publications include conference proceedings, monographs, data compilations, handbooks, sourcebooks, and special bibliographies.

TECHNOLOGY UTILIZATION PUBLICATIONS: Information on technology used by NASA that may be of particular interest in commercial and other non-aerospace applications. Publications include Tech Briefs, Technology Utilization Reports and Technology Surveys.

Details on the availability of these publications may be obtained from:

SCIENTIFIC AND TECHNICAL INFORMATION OFFICE

NATIONAL AERONAUTICS AND SPACE ADMINISTRATION
Washington, D.C. 20546